Wetlands (2011) 31:377–387
DOI 10.1007/s13157-011-0147-x

ARTICLE

Water Sources and Hydrodynamics of Closed-Basin Depressions, Cook Inlet Region, Alaska

Mark C. Rains

Received: 2 October 2010 / Accepted: 5 January 2011 / Published online: 22 March 2011

Abstract Among the most prevalent wetland and deep-water habitats in Alaska are ponds, many of which are subarctic ponds occurring as moraine, ice-scour, or dead-ice depressions. Many are closed-basin depressions, where surface-water inflows and outflows are negligible. The objective of this study was to quantify the water sources and hydrodynamics of these subarctic ponds, particularly with respect to the role they play in groundwater recharge. There are two types of ponds on the study site. Perched-precipitation ponds have inflows by melt water and direct precipitation, outflows by evapotranspiration and groundwater recharge, and are seasonally inundated because surface water is perched above the water table and infiltration through the low-permeability surficial deposits to the water table is slow. Flow-through ponds have inflows by melt water, direct precipitation, and groundwater discharge, outflows by evapotranspiration and groundwater recharge, and are perennially inundated because of groundwater throughflow. Both are groundwater recharge focal points. This is particularly true for perched-precipitation ponds, where net groundwater recharge rates were 215% larger than in flow-through ponds, and 332% larger than in the broader landscape. Most of the additional groundwater recharge occurs immediately following breakup, as aeolian-transported snow trapped in the depressions melts which results in enhanced groundwater recharge rates.

Keywords Glacial environments · Groundwater recharge · Subarctic ponds · Wetland and deep-water habitats · Wetland hydrology

M. C. Rains (✉)
Department of Geology, University of South Florida,
Tampa, FL 33620, USA
e-mail: mrains@usf.edu

Introduction

Wetland and deep-water habitats cover >50% of the land surface in Alaska (Hall et al. 1994), performing a variety of functions such as providing habitat for migratory birds (DeGraaf and Rappole 1995), including approximately 70,000 swans, one million geese, and 12 million ducks annually (Hall et al. 1994). Ponds are among the most prevalent and noticeable wetland and deep-water habitats in Alaska (Hall et al. 1994; Prowse et al. 2006). In subarctic Alaska, ponds typically occur as moraine, ice-scour, or dead-ice depressions on the undulating, often low-permeability terrain (Prowse et al. 2006). Many of these ponds are closed-basin depressions, where surface-water inflows and outflows are negligible (Ferone and Devito 2004; Prowse et al. 2006). Such ponds are particularly common in the Cook Inlet Region of Alaska, where numerous Pleistocene and Holocene glacial advances have been recorded (Karlstrom 1964). Little hydrologic research has been conducted on these common systems, with most research instead focused on ponds occurring as thermokarst depressions in arctic Alaska (e.g., Marsh and Woo 1977; Woo et al. 1981; Woo and Guan 2006). Therefore, little is known about the hydrologic processes in subarctic ponds, which makes it difficult to predict the potential effects of land-use change, such as urban development, oil and gas exploration, mining, agriculture, forest practices (State of Alaska 2004), and climate change, such as a drying trend that has been observed in both south-central and interior Alaska (Klein et al. 2005; Corcoran et al. 2009).

The objective of this study was to quantify the water sources and hydrodynamics of these subarctic ponds, particularly with respect to the role they play in groundwater recharge. This study was guided by the hypothesis that there are two types of ponds which differ with respect to water sources and hydrodynamics: (1) perched-precipitation ponds, which have inflows by melt water and direct precipitation, outflows by evapotranspiration and groundwater recharge, and are seasonally inundated because surface water is perched above the water table and infiltration through the low-permeability surficial deposits to the local water table is slow, and (2) flow-through ponds, which have inflows by melt water, direct precipitation, and groundwater discharge, outflows by evapotranspiration and groundwater recharge, and are perennially inundated because of the groundwater throughflow.

Study Area

The study site is a ~101,000-hectare area located west of Cook Inlet, southwest of Lake Clark and north of Lake Iliamna, in southwest Alaska (Fig. 1). The study site is in the Nushagak-Big River Hill physiographic division, which is characterized by low, rolling hills separated by wide, shallow valleys (Wahrhaftig 1965), and is near the southern boundary of the discontinuous permafrost zone of Alaska (Péwé 1975), although field observations suggest that wet permafrost is lacking. The predominant vegetation is scrub-shrub, largely composed of various combinations dwarf trees and tall, low, and dwarf shrubs (Viereck et al. 1992).

The study site is primarily underlain by Upper Cretaceous-Tertiary intrusive rocks including granodiorite, quartz monzonite, and quartz diorite, which are partially covered by Tertiary and Quaternary volcanic and sedimentary rocks and deposits (Detterman and Reed 1973b). There were at least four major Pleistocene glacial advances in the last 39,000 years (Detterman and Reed 1973a; Mann and Peteet 1994; Stilwell and Kaufman 1996; Hamilton and Klieforth 2010). These glacial advances left complex surficial deposits, including arcuate end moraines enclosing irregular, hummocky ground moraines; linear lateral moraines on the lower elevations of valley sidewalls; irregular, hummocky ice-contact melt-water deposits; and pitted outwash plains and valley trains extending down valley from end moraines. Moraine, ice-scour, and/or dead-ice depressions are prominent features in many of these deposits.

This study was conducted in two phases. In the first phase, seven ponds located in three different hydrogeologic regions were studied. At the northernmost site, there were two ponds classified *a priori* as flow-through ponds located in relatively high-gradient lateral moraine deposits; at the middle site, there were two ponds classified *a priori* as perched-precipitation ponds located in low-gradient ground moraine deposits; and at the southernmost site, there were two ponds classified *a priori* as flow-through ponds and one pond classified *a priori* as a perched-precipitation pond located in ground moraine deposits (Fig. 1). There were no surface-water outflows from any of the ponds, except for a

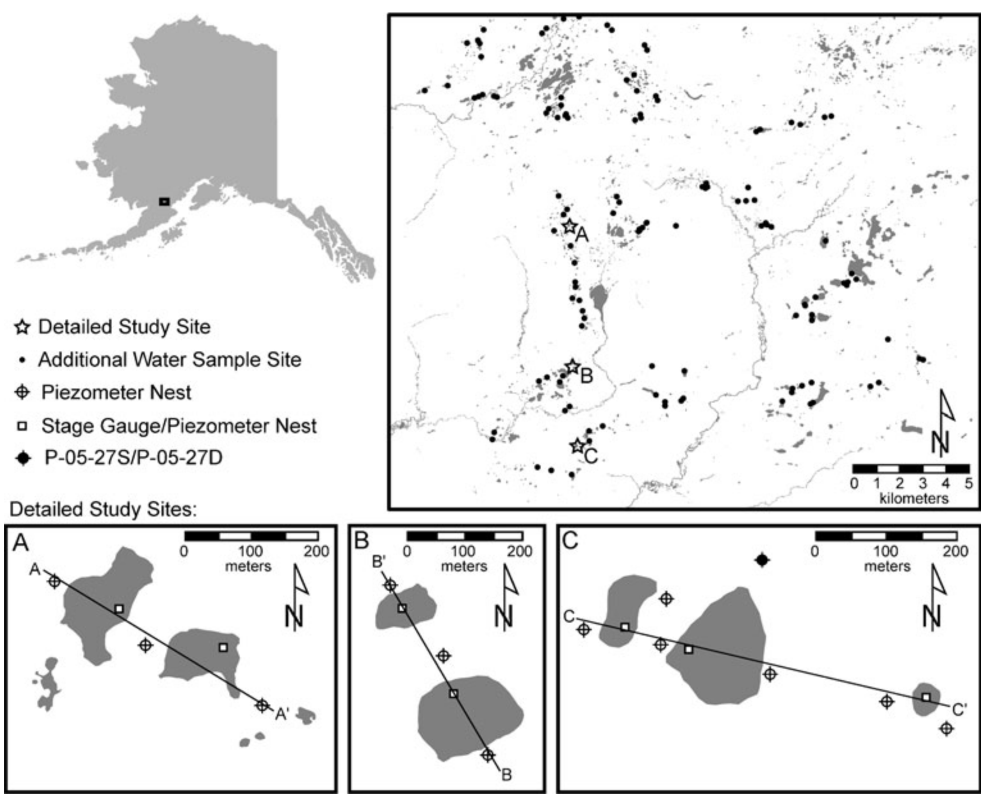

Fig. 1 Location of the study site and the detailed study sites, instrumentation at the seven ponds located at the detailed study sites, and locations where water samples were collected at the 123 additional ponds located throughout the study site. The three stars in the uppermost inset refer to the detailed study sites shown in the lowermost insets. A-A', B-B', and C-C' in the lowermost insets delineate the locations of cross sections. P-05-27 S/P-05-27D refers to a nest of a shallow and a deep monitoring well installed at the southernmost site prior to the initiation of this study

small surface-water connection between the two flow-through ponds at the southernmost site. Multiple slug tests indicated that the saturated hydraulic conductivity of the surficial deposits around the ponds was on the order of 10^{-8} cm/s, which is consistent with expected values for glacial till (Freeze and Cherry 1979). The southernmost site was located just south of a hypothesized groundwater divide between the South Fork Koktuli Basin to the north and the Upper Talarik Basin to the south (Smith pers. comm. 2009a). In the second phase, 123 additional ponds located throughout the study site were studied. Of these 123 additional ponds, 45 were classified *a priori* as perched-precipitation ponds and 78 were classified *a priori* as flow-through ponds.

Methods

Classification

All ponds were classified *a priori* as either perched-precipitation ponds or flow-through ponds. Ponds with specific conductances of <20 μS/cm and with stages that generally declined and exposed unvegetated margins by middle-late summer were classified as perched-precipitation ponds, while ponds with specific conductances of ≥20 μS/cm and with stages that were stable and had vegetated margins throughout summer were classified as flow-through ponds. A very small number of ponds had specific conductances of ≥20 μS/cm but unvegetated margins, and therefore did not fit this classification scheme. These ponds were classified as flow-though ponds based only upon specific conductance, and one of these special-case ponds was included in the first phase of this study.

Chemical Hydrology

In June and August 2006, precipitation, surface-water, and groundwater samples were collected at the seven ponds located at the three detailed study sites (Fig. 1). In August 2007, precipitation, surface-water, and groundwater samples were collected at the seven ponds located at the three detailed study sites and surface-water samples were collected at the 123 additional ponds located throughout the study site (Fig. 1). Precipitation samples were collected from late-spring snowfields and summer rainfall collectors. In total, 179 water samples were collected, not including duplicate and triplicate water samples used for quality assurance and quality control.

In the field, all samples were filtered through 0.45 μm polycarbonate membranes and placed in 125 mL HDPE bottles. All tubing was rinsed with native water between samplings. Piezometers were purged before samples were collected. Cation sample bottles were pre-acidified with 1 mL of nitric acid. All samples were stored at 4±2°C prior to analyses.

Temperature, specific conductance, and pH were measured in the field using a YSI 556 MPS (YSI, Inc., Yellow Springs, Ohio) or the equivalent. Sodium, potassium, magnesium, calcium (Na^+ [0.10], K^+ [0.05], Mg^{2+} [0.02], and Ca^{2+} [0.05] [detection limit ppm]), and silica (SiO_2 [0.10] [detection limit ppm]) were measured with inductively coupled plasma-atomic emission spectroscopy by the EPA 200.7 or 200.8 methods (Clesceri et al. 1998). Chloride and sulfate (Cl^- [0.20] and SO_4^{2-}[0.20] [detection limit ppm]) were measured with ion chromatography by the EPA 300.0 or EPA 375.2 methods (Clesceri et al. 1998). Carbonate alkalinity was back-calculated by assuming all other cations and anions were measured, and that bicarbonate accounted for the entire missing charge in charge balance error analyses. Quality assurance was provided by the primary laboratory (SGS Environmental Services, Inc., Anchorage, Alaska) through the analysis of duplicate water samples for ~20% of the total water samples, while quality control was provided by the quality-control laboratory (Columbia Analytical Services, Inc., Kelso, Washington) through the analysis of triplicate water samples for ~10% of the total water samples. Analytical precisions were typically better than 1%.

Solute concentrations can increase by evapoconcentration (i.e., the process by which solute concentrations increase as water evaporates and solutes are retained in the remaining solution) and/or by water-rock interaction (i.e., the process by which solute concentrations increase as deposits dissolve in water). Regional sediments are largely derived from granodiorite, quartz monzonite, and quartz diorite, which contain high concentrations of sodium, potassium, magnesium, calcium, and silica but no chloride. Therefore, silica and chloride were used as conservative natural tracers in both evapoconcentration and water-rock interaction models to determine if the observed differences in solute concentrations in the pond surface waters could be explained by evapoconcentration of precipitation or water-rock interaction between precipitation and regional sediments.

The evapoconcentration model was

$$C_{RES} = \frac{C_{INI}}{f_{RES}}$$

where C is the silica or chloride concentration in ppm, f is the fraction of water remaining as it evaporates, and the subscripts *RES* and *INI* refer to residual water (e.g., evaporated surface water in the ponds) and initial water (e.g., precipitation), respectively. Precipitation was assigned mean silica and chloride concentrations calculated from nine precipitation samples and theoretically evaporated in a stepwise fashion with f_{RES} set to 1.00, 0.75, 0.50, and 0.25. The water-rock interaction model was run in PHREEQC Interactive Version 2.17.1.4468 (Parkhurst and Appelo 1999). Precipitation was assigned mean silica and chloride concentrations calculated from nine precipitation samples and allowed to equilibrate with minerals common to regional sediments (i.e., feldspar and quartz) at the mean groundwater temperature and pH of 7°C and 7.5, respectively.

Physical Hydrology

Physical hydrology data were collected at the seven ponds located at the three detailed study sites (Fig. 1). Precipitation was measured continuously at each of the three detailed study sites, while net radiation, temperature, relative humidity, and wind speed were measured hourly at one location within ~1–10 km of each of the three detailed study sites. Precipitation was measured with HOBO Data Logging Rain Gauges (Onset Computer Corporation, Bourne, Massachusetts), solar radiation was measured with a LI200X Silicon Pyranometer (LI-COR, Inc., Lincoln, Nebraska), temperature was measured with a Model 062 Air Temperature Sensor (Met One, Inc., Grants Pass, Oregon), relative humidity was measured with a HMP45C-L Vaisala Temperature and RH Probe (Vaisala, Inc., Boulder, Colorado), and wind speed was measured with a F460 Wind Speed Sensor (Climatronics, Inc., Davenport, Iowa). Other meteorological variables were parameterized as necessary using standard procedures (Allen et al. 2005).

Daily reference evapotranspiration, ET_o, was computed using the ASCE Standardized Reference Evapotranspiration Equation (Allen et al. 2005). The ASCE Standardized Reference Evapotranspiration Equation is a slight modification of the FAO Penman-Montieth Equation (Doorenbos and Pruitt 1977), and the two equations produce nearly identical results (Gavilán et al. 2008). The ASCE Standardized Reference Evapotranspiration Equation is

$$ET_o = \frac{0.408\Delta(Rn - G) + \gamma \frac{900}{T+273} U_2(e_s - e_a)}{\Delta + \gamma(1 + 0.34U_2)}$$

where ET_o is reference evapotranspiration (mm/d), Δ is the slope vapor pressure curve (kPa/°C), Rn is net radiation (MJ/m^{2}day), G is soil heat flux density (MJ/m^{2}day), γ is the psychrometric constant (kPa/°C), T is temperature (°C), U_2 is the wind speed (m/s), e_s is mean saturation vapor pressure (kPa), and e_a is actual vapor pressure (kPa). Working in a variety of climates in the western USA and southern Europe, Ventura et al. (1999) showed that the root mean square of ET_o computed with the FAO Penman-Montieth Equation with respect to ET_o measured in lysimeters was consistently ~0.4 mm/d. This was ~25% of the mean daily ET_o and an order of magnitude smaller than other key terms in the water budget during the course of this study. Actual ET was assumed to be equal to ET_o throughout the summer because the ponds are either open water, fully-wet sediments, or fully-wet, laterally-extensive short vegetation (Allen et al. 2005).

Stages (i.e., surface-water levels) were measured hourly with Model 3001 Levelogger Gold pressure transducers and dataloggers (Solinst, Inc., Georgetown, Ontario). Hydraulic heads were measured at piezometer nests, with two piezometers in each nest. Each piezometer was constructed of stainless steel pipe with an inside diameter of ~5 cm. Both piezometers were screened over ~50 cm with 0.010 slot size screens, with screening beginning ~1.5 m or ~3.0 m below the ground surface. Piezometers were installed by drilling boreholes with a borehole auger, placing the piezometers in the boreholes, and filling the annulus with sand to above the screened intervals and then bentonite to above the ground surface. Hydraulic heads (i.e., groundwater levels) were measured monthly with a Model 101 Water Level Indicator (Solinst, Georgetown, Ontario) or the equivalent. Time-lag errors can arise in piezometers screened in low-conductivity formations (Hanschke and Baird 2001). The potential for time-lag errors was minimized by summarizing hydraulic heads over long time steps.

Net groundwater recharge through the ponds to the broader hydrological landscape was computed with a water-budget approach. Water budgets were computed from the water-budget equation where

$$P - ET + \Delta SW + \Delta GW = \Delta S$$

and where P is precipitation, ET is evapotranspiration, ΔSW is net surface water inflow (i.e., surface-water inflow–surface-water outflow), ΔGW is net groundwater inflow (i.e., groundwater inflow–groundwater outflow), and ΔS is the change in storage (i.e., the change in stage). Surface-water inflows and outflows were negligible. This includes overland flows, which were negligible because annual frost increases vertical permeability which facilitates the rapid infiltration of summer precipitation (Chamberlain and Gow 1979). Therefore, the water-budget equation could be re-written and resolved in terms of net groundwater inflow where

$$\Delta GW = \Delta S - P + ET$$

and where terms are as previously defined. This conceptualization assumes that the effective specific yield of the ponds was unity. This is generally true where stages are well-above land surface (Sumner 2007), which was generally the case for these ponds throughout the period of record. Net groundwater inflow was computed on daily time steps to determine the net groundwater recharge from the ponds to the underlying aquifers during June–September.

Results

Chemical Hydrology

In general, solute concentrations were lowest in precipitation and perched-precipitation pond surface water and ground water, and highest in flow-through pond surface water and ground water (Table 1). Mean±SD specific conductances were 7±3, 18±7, 28±8, and 67±44 μS/cm for surface water in the perched-precipitation ponds, ground water underneath the perched-precipitation ponds, surface water in the flow-through ponds, and ground water underneath and adjacent to the flow-through ponds, respectively. Mean±SD solute concentrations were generally lower in the perched-precipitation pond surface water than in the flow-through pond surface water, with Student's *t*-tests indicating that these differences were significant for the conservative solutes sodium (0.68±0.18 v. 1.61±0.50 ppm, $p<0.01$), magnesium (0.13±0.03 v. 1.02±0.37 ppm, $p<0.01$), calcium (0.41±0.14 v. 4.19±1.32 ppm, $p<0.01$), and silica (0.14±0.06 v. 1.20±1.18 ppm, $p=0.02$), but not for the conservative solute chloride (0.73±0.16 v. 0.64±0.16 ppm, $p=0.22$).

Silica and chloride concentrations measured in the perched-precipitation ponds and flow-through ponds show that flow-through ponds are preferentially enriched with silica (Fig. 2). The evapoconcentration model shows that evapoconcentration would result in the proportional enrichment of both silica and chloride, while the water-rock interaction model shows that water-rock interaction would result in preferential enrichment of silica. Therefore, these measured and modeled results indicate that ground water discharges to the flow-through ponds but not to the perched-precipitation ponds to any significant degree. A two-endmember mixing line with magnesium and calcium indicates that precipitation, surface water in the perched-precipitation ponds, ground water underneath the perched-precipitation ponds, surface water in the flow-through ponds, and ground water underneath and adjacent to the flow-through ponds occur on a continuum, with precipitation and ground water underneath and adjacent to the flow-through ponds as the two endmembers (Fig. 3).

Patterns observed in the ponds at the detailed study sites also were observed in the 123 additional ponds located throughout the study site (Table 2). In general, solute concentrations were lowest in the perched-precipitation pond surface water and highest in the flow-through pond surface water. Mean±SD specific conductances were 11±5 and 48±24 μS/cm for surface water in the perched-precipitation ponds and surface water in the flow-through ponds, respectively. Mean±SD solute concentrations were generally lower in the perched-precipitation ponds than in the flow-through ponds, with Student's *t*-tests indicating that these differences were significant for the conservative solutes sodium (0.75±0.30 v. 2.14±0.85 ppm, $p<0.01$), magnesium (0.27±0.16 v. 1.39±0.96 ppm, $p<0.01$), calcium (1.02±0.74 v. 5.93±3.22 ppm, $p<0.01$), and silica (0.41±0.67 v. 1.68±1.49 ppm, $p<0.01$), but not for the conservative solute chloride (0.42±0.15 v. 0.40±0.18 ppm, $p=0.48$).

The basic mass-balance mixing relationship observed in the surface water in the ponds at the detailed study sites also was observed in the surface water in the 123 additional

Table 1 Specific conductance, pH, and solute concentrations of water samples collected from the seven ponds located at the detailed study sites. Values are means (± standard deviations) for precipitation; surface water and groundwater samples from perched-precipitation ponds; and surface water and groundwater samples from flow-through ponds. Groundwater samples were collected from underneath the perched-precipitation ponds and underneath and adjacent to the flow-through ponds

Constituent	Precipitation (n=9)	Perched-precipitation ponds		Flow-through ponds	
		Surface water (n=9)	Ground water (n=5)	Surface water (n=12)	Ground water (n=21)
SC (μS/cm)	–	7 (± 3)	18 (± 7)	28 (± 8)	67 (± 44)
pH	–	7.4 (± 1.5)	7.5 (± 1.8)	7.8 (± 0.5)	7.4 (± 0.7)
Na (ppm)	0.58 (± 0.45)	0.68 (± 0.18)	1.89 (± 0.59)	1.61 (± 0.50)	5.15 (± 5.38)
K (ppm)	0.48 (± 0.50)	0.27 (± 0.08)	0.56 (± 0.26)	0.37 (± 0.13)	0.81 (± 0.43)
Mg (ppm)	0.11 (± 0.08)	0.13 (± 0.03)	0.40 (± 0.15)	1.02 (± 0.37)	2.27 (± 1.71)
Ca (ppm)	0.59 (± 0.25)	0.41 (± 0.14)	1.59 (± 0.64)	4.19 (± 1.32)	9.13 (± 5.68)
Cl (ppm)	0.77 (± 0.66)	0.73 (± 0.16)	1.14 (± 0.18)	0.64 (± 0.16)	1.07 (± 0.68)
SO_4 (ppm)	0.62 (± 0.34)	0.66 (± 0.54)	1.02 (± 0.44)	3.20 (± 0.95)	6.94 (± 6.44)
Alkalinity (ppm)	2.52 (± 1.58)	1.87 (± 0.65)	9.45 (± 3.71)	17.57 (± 5.88)	43.49 (± 34.70)
SiO_2 (ppm)	0.09 (± 0.06)	0.14 (± 0.06)	4.92 (± 3.25)	1.20 (±1 .18)	5.72 (± 3.26)

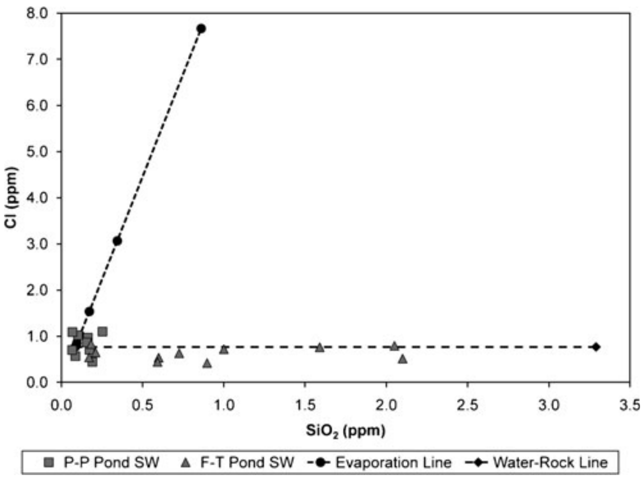

Fig. 2 Measured and modeled silica and chloride concentrations in surface water at the perched-precipitation ponds (P-P Pond SW) and flow-through ponds (F-T Pond SW) located at the detailed study sites. The modeled Evaporation Line represents the trajectory on which the residual water would trend, with solid circles representing modeled points at f=1.00, 0.75, 0.50.and 0.25. The modeled Water-Rock Line represents the trajectory on which water in contact with regional sediments would trend as it moved toward the equilibrium condition

ponds located throughout the study site (Fig. 4). Least-squares regression lines for magnesium v. calcium were

$$y = 0.22x + 0.07$$

for both surface water in the ponds at the detailed study sites and for the surface water in the 123 additional ponds located throughout the study site. Both relationships were significant, with $p<0.01$ for both ponds at the detailed study sites and the 123 additional ponds located throughout the study site. However, variability was greater in the 123 additional ponds located throughout the study site, with R^2=0.83 and R^2=0.68

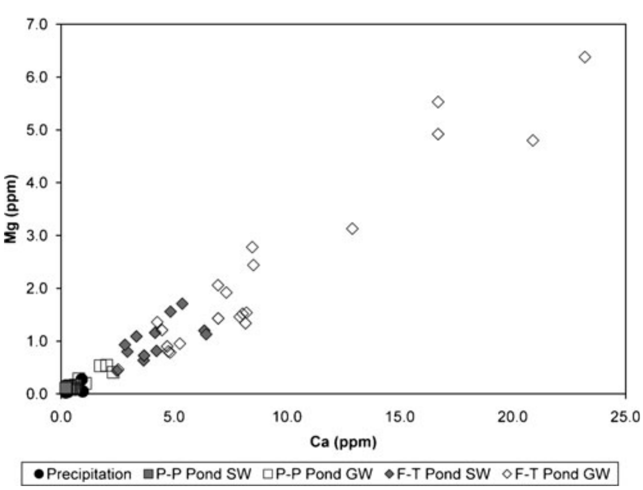

Fig. 3 Two-endmember surface-water and groundwater mixing line for surface water and ground water at the perched-precipitation ponds (P-P Pond SW and P-P Pond GW, respectively) and the flow-through ponds (F-T Pond SW and F-T Pond GW, respectively) located at the detailed study sites

Table 2 Specific conductance, pH, and solute concentrations of water samples collected from the 123 additional ponds located throughout the study site. Values are means (± standard deviations) for surface-water samples collected from perched-precipitation and flow-through ponds

Constituent	Perched-precipitation ponds (n=45)	Flow-through ponds (n=78)
SC (μS/cm)	11 (± 5)	48 (± 24)
pH	7.0 (± 0.6)	7.2 (± 0.3)
Na (ppm)	0.75 (± 0.30)	2.14 (± 0.85)
K (ppm)	0.24 (± 0.12)	0.36 (± 0.32)
Mg (ppm)	0.27 (± 0.16)	1.39 (± 0.96)
Ca (ppm)	1.02 (± 0.74)	5.93 (± 3.22)
Cl (ppm)	0.42 (± 0.15)	0.40 (± 0.18)
SO_4 (ppm)	0.37 (± 0.51)	2.97 (± 6.97)
Alkalinity (ppm)	5.64 (± 3.35)	26.84 (± 12.88)
SiO_2 (ppm)	0.41 (± 0.67)	1.68 (± 1.49)

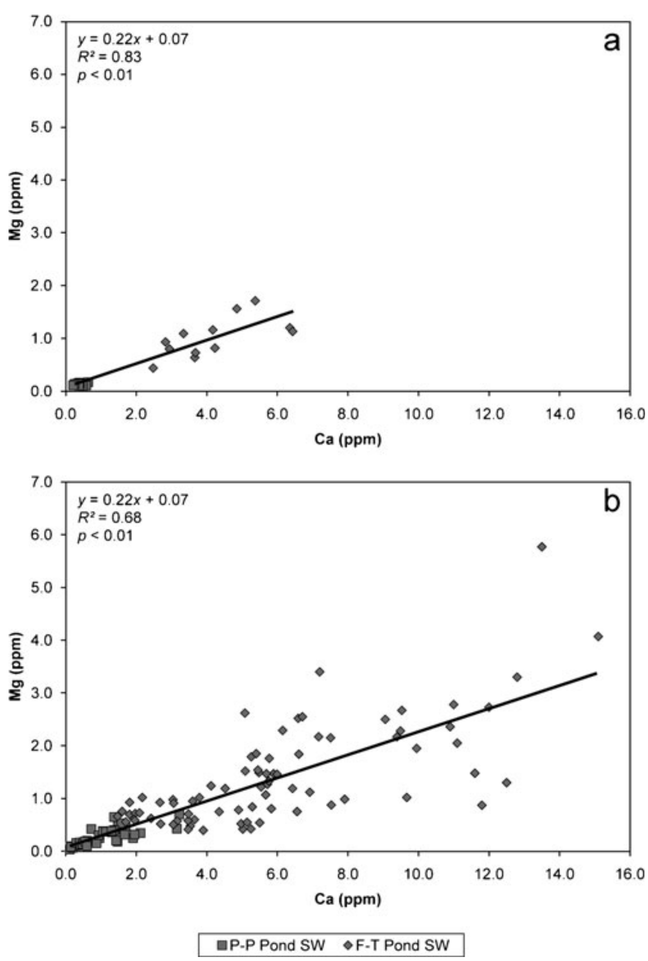

Fig. 4 Two-endmember mixing lines for surface water from the perched-precipitation ponds (P-P Pond SW) and flow-through ponds (F-T Pond SW) located at **a** the detailed study sites and **b** the 123 additional study sites located throughout the study area

for the ponds at the detailed study sites and the 123 additional ponds located throughout the study site, respectively.

Physical Hydrology

The perched-precipitation ponds and flow-through ponds had different hydrographic characteristics (Fig. 5). The perched-precipitation ponds were at full pool immediately following breakup in late May/early June. Precipitation was relatively infrequent and of low intensity in June and July. During this time, the perched-precipitation pond stages declined an average of 1.35 cm/d until they were nearly empty and had large, unvegetated margins by late July. Precipitation increased in frequency and intensity in August and September. During this time, the perched-precipitation pond stages increased slightly then remained relatively low but stable through September. Conversely, three of the four flow-through ponds (hereafter referred to as typical flow-through ponds) were at full pool throughout the summer, showing little to no effect from breakup in late May/early June, the relatively low frequency and intensity precipitation in June and July, or the relatively high frequency and intensity precipitation in August and September. The fourth flow-through pond was a special-case flow-through pond, with a stage that was intermediate between the hydraulic head in an up-gradient local, perched flow system and an underlying regional, confined flow system (Fig. 6). Spearman's rank correlation indicated that mean daily stages were uncorrelated in a comparison of perched-precipitation ponds and typical flow-through ponds (r_s (118)=0.03, p=0.77) and in a comparison of typical flow-through ponds and the one special-case flow-through pond (r_s (77)=0.13, p=0.27), and were only weakly correlated in a comparison of perched-precipitation ponds and the one special-case flow-through pond (r_s (77)=0.26, p=0.02).

Ground water was not observed in piezometers directly adjacent to the perched-precipitation ponds but was observed in all piezometers under the perched-precipitation ponds.

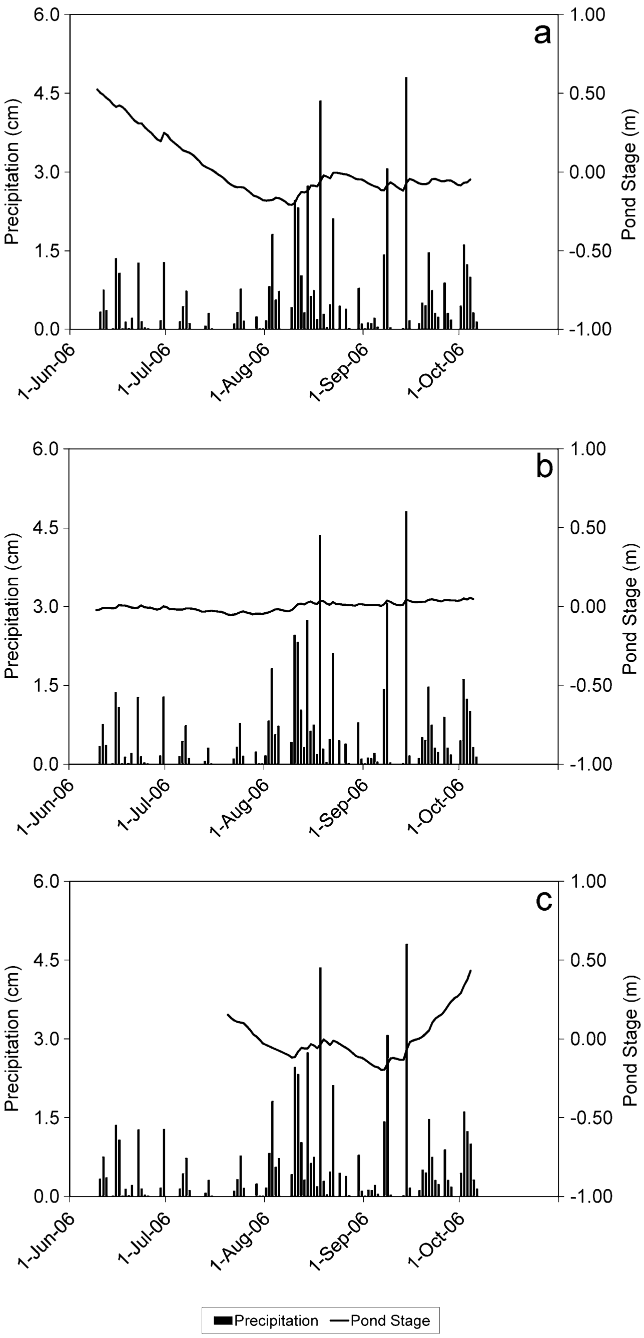

Fig. 5 Precipitation and relative pond stage in **a** the perched-precipitation ponds (mean, n=3), **b** the typical flow-through ponds (mean, n=3), and **c** the special-case flow-through pond (n=1). Pond stages are relative to mean pond stage from June–September

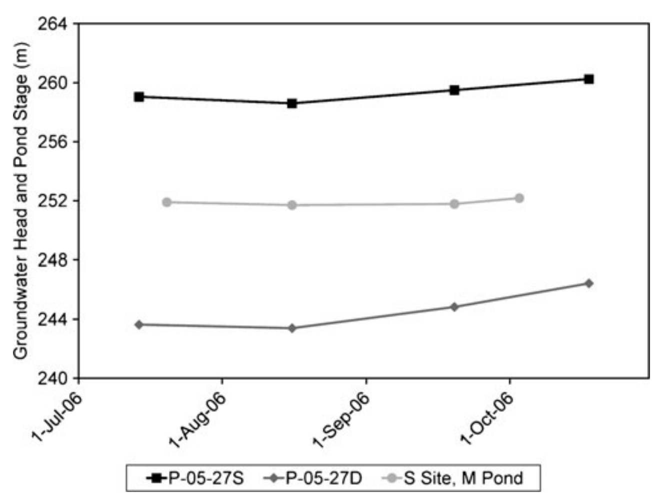

Fig. 6 Relationship between stage in the special-case flow-through pond and head in the local and regional flow systems located at the southernmost detailed study site. Water appears to flow from an up-gradient local, perched flow system (e.g., P-05-27 S), through the flow-through ponds (e.g., S Site, M Pond), and into the underlying regional, confined flow system (e.g., P-05-27D). Data from the P-05-27 S and P-05-27D are from unpublished data (Smith, pers. comm., 2009a)

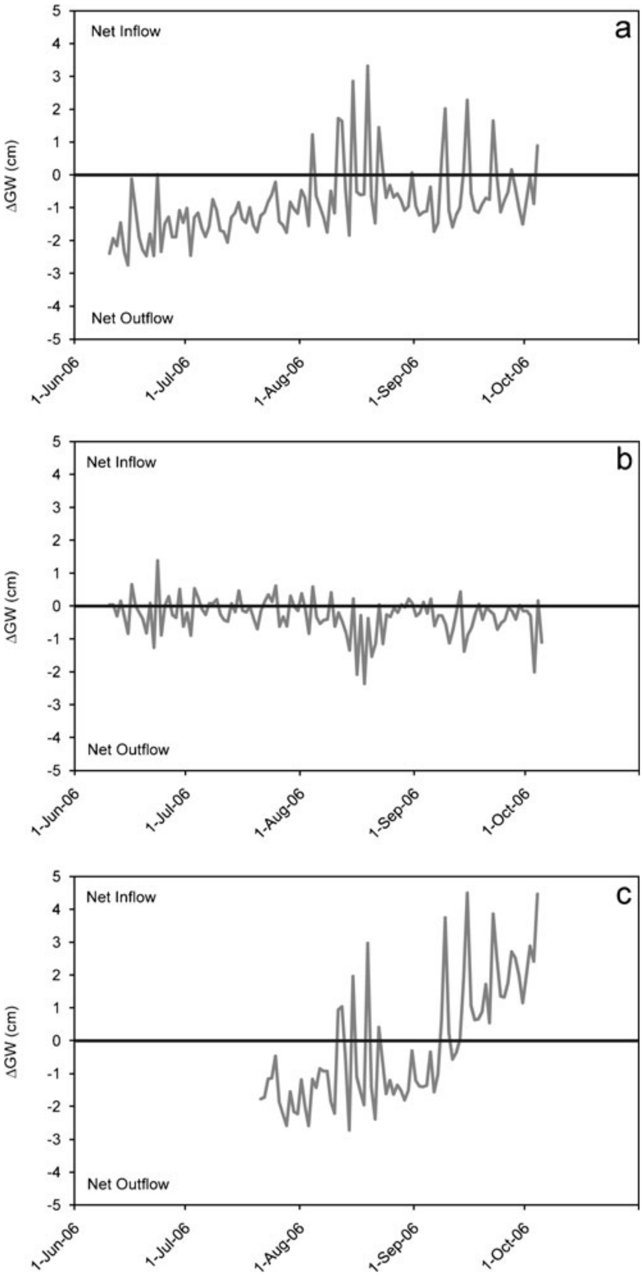

Fig. 7 Net groundwater recharge in **a** the perched-precipitation ponds (mean, $n=3$), **b** the typical flow-through ponds (mean, $n=3$), and **c** the special-case flow-through pond ($n=1$)

Where found, hydraulic gradients were down, indicating that groundwater recharge occurred through the perched-precipitation ponds. Ground water was observed in piezometers up gradient, underneath, and down gradient of the flow-through ponds indicating that ground water flowed through the flow-through ponds, with groundwater discharge occurring at the up-gradient ends of the flow-through ponds and groundwater recharge occurring at the down-gradient ends of the flow-through ponds. Where ground water was present, it remained unfrozen through the winter in only three locations, all of which were adjacent to or underneath flow-through ponds.

Groundwater recharge occurred through both perched-precipitation ponds and flow-through ponds (Fig. 7). However, patterns and amounts differed. In the perched-precipitation ponds, net groundwater recharge rates were greatest in the early summer immediately following breakup, then decreased but remained relatively high throughout the summer. In the typical flow-through ponds, net groundwater recharge rates were lower and relatively uniform throughout the summer. In the one special-case flow-through pond, net groundwater recharge occurred in the early summer, while net groundwater discharge occurred in the late summer. Although the patterns differed, a Student's *t*-test indicated that net groundwater recharge rates were not significantly different between the average condition at the typical flow-through ponds and the conditions at the one special-case flow through pond ($p=0.48$). Combining the records from all four flow-through ponds, mean±SD groundwater recharge during June–September for the perched-precipitation ponds and flow-through ponds was 0.82±1.12 and 0.26±0.97 cm/d, respectively (Table 3). A Student's *t*-test indicated that daily groundwater recharge rates were significantly higher in the perched-precipitation ponds than in the flow-through ponds ($p<0.01$).

Discussion

Results indicate that there are two types of ponds: perched-precipitation ponds and flow-through ponds. Although they look similar, and were formed by similar processes, these two types of ponds differ with respect to their water sources and hydrodynamics.

Perched-precipitation ponds have inflows by melt water and direct precipitation, outflows by evapotranspiration and groundwater recharge, and are seasonally inundated because surface water is perched above the local water table and infiltration through the low-permeability surficial deposits to the local water table is slow (Fig. 8). These ponds are typically located where groundwater discharge is unlikely to

Table 3 Net groundwater recharge through the seven ponds located at the detailed study sites. Values are mean (± standard deviation) and maximum groundwater recharge through perched-precipitation and flow-through ponds during June–September. Mean groundwater recharge on the study site was ~0.19 cm/d during June–September (Smith, pers. comm., 2009a)

	Perched-precipitation ponds	Flow-through ponds
Mean (±SD) (cm/d)	0.82 (± 1.12)	0.26 (± 0.97)
Maximum (cm/d)	2.78	2.28

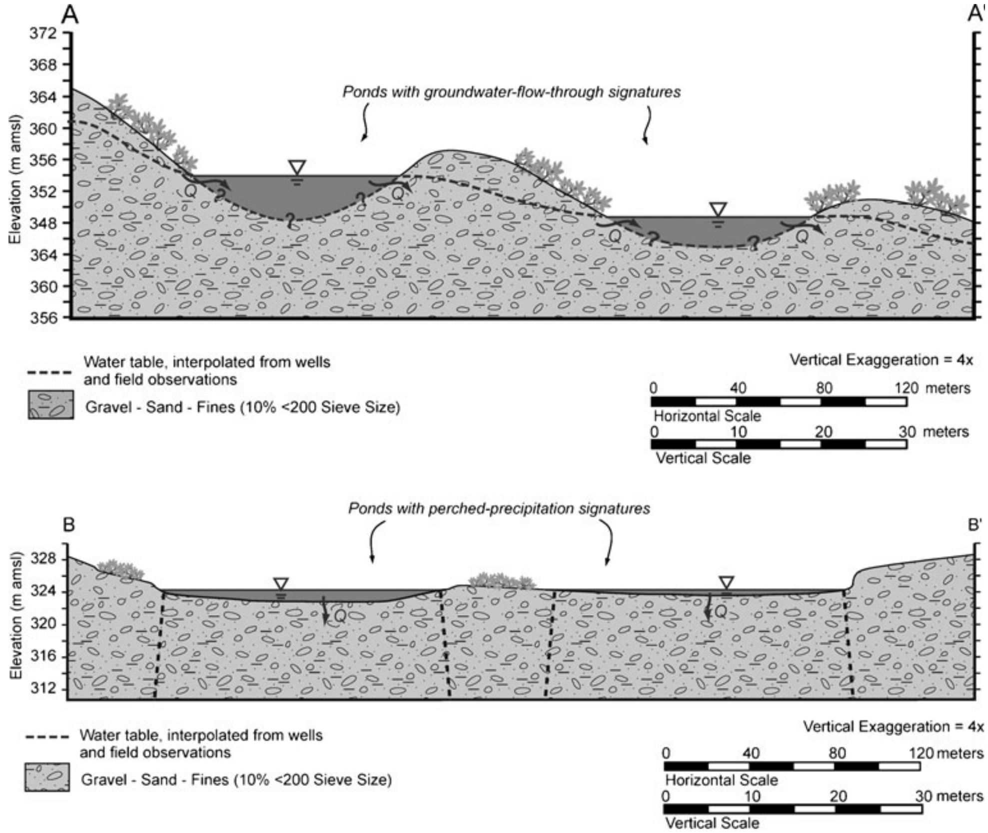

Fig. 8 Conceptual model of the physical hydrology of the flow-through ponds located at the northernmost detailed study site (A-A') and the perched-precipitation ponds located at the middle detailed study site (B-B')

occur (e.g., shallow ponds in nearly-level ground moraine) and typically have wide, unvegetated margins by middle-late summer. Surface water has geochemical characteristics of precipitation, while ground water underneath these ponds has geochemical characteristics of precipitation that has undergone slight modification due to short-term water-rock interaction (Tables 1 and 2, Figs. 2, 3 and 4).

The groundwater recharge analysis suggests that ground water periodically discharges to the perched-precipitation ponds (Fig. 7). However, all apparent groundwater discharge events occurred on days when precipitation was >1.5 cm/d. On these days, rainfall intensity could have exceeded infiltration capacity, generating overland flow which would have violated the assumption that surface-water inflow was negligible. Therefore, these apparent groundwater discharge events could instead have been ephemeral surface-water inflow events.

Flow-through ponds have inflows by melt water, direct precipitation, and groundwater discharge, outflows by evapotranspiration and groundwater recharge, and are perennially inundated because of the groundwater throughflow (Fig. 8). These ponds are typically located where groundwater discharge is likely to occur (e.g., deep ponds on gently- to strongly-sloping lateral moraines) and typically have stable, vegetated margins throughout summer. Surface water has geochemical characteristics of mixed precipitation and ground water, while ground water has geochemical characteristics of precipitation that has undergone slight modification due to short-term water-rock interaction (Tables 1 and 2, Figs. 2, 3 and 4).

One flow-through pond at the detailed study sites had a distinct hydrograph, with a stage that was intermediate between the hydraulic head in the up-gradient local, perched flow system and down-gradient in the underlying regional, confined flow system (Fig. 6). Although a flow-through pond, this pond had a wide, unvegetated margin immediately following breakup, which became increasingly flooded toward the middle-late summer. This pond was of unknown depth; the bottom could not be seen even from the air, in spite of the fact that the water was quite clear. This type of pond appears to be an uncommon variant of the broader class of flow-through ponds, in which the pond is deep enough to penetrate through or largely through the low-permeability surficial deposits, such as ground-moraine deposits, and into or close to the underlying high-permeability deposits, such as buried advance outwash deposits. These ponds are connected to local, perched flow systems, but stages can be at least partly controlled by hydraulic heads in the underlying regional, confined flow systems. This appears to be the case for this pond. Immediately following breakup, local groundwater discharged to the pond from numerous seeps and springs, but stage in the pond nevertheless rapidly declined, indicating that groundwater recharge from the pond far exceeded groundwater discharge to the pond (Figs. 5 and

7). In the late summer, ground water apparently spilled over a bedrock sill and thereafter flowd from the South Fork Koktuli Basin located to the north of the pond to the Upper Talarik Basin located south of the pond, passing through the buried advance outwash deposits that are ~40 m below the full-pool water surface of the pond (Smith pers. comm. 2009a). When this apparently occurred, groundwater discharge to the pond far exceeded groundwater recharge from the pond and stage in the pond rapidly rose (Figs. 5, 6 and 7).

Regardless, the flow-though ponds are surface-water expressions of local and/or regional groundwater flows. Flow-through lakes and depressional wetlands have long been recognized. Born et al. (1979) described flow-though lakes, while Sloan (1972) and Richardson et al. (1992) described flow-through prairie potholes. More recently, Rains et al. (2006) showed that vernal pools in central California are a special case, being flow-though wetlands supported by a seasonal perched aquifer that is unconnected to the underlying regional aquifers.

Both types of ponds are depressional features that collect and store water and serve as focal points for groundwater recharge, which is often the case for closed-basin depressions located on till and moraine deposits (Meyboom 1966; van der Kamp and Hayashi 1998; Dempster et al. 2006; Todd et al. 2006). An ongoing, regional-scale water-budget study indicated that mean groundwater recharge during the course of the study was ~0.19 cm/d (Smith pers. comm. 2009b), which is consistent with regional-scale estimates of groundwater recharge in other till and moraine landscapes (Saxena 1984; Johansson 1987; Labadia and Buttle 1996; Bauer and Mastin 1997). Therefore, groundwater recharge rates were 332% larger in the perched-precipitation ponds and 37% larger in the flow-through ponds than on the broader landscape during the course of the study (Table 3, Fig. 7).

Groundwater recharge is particularly pronounced in perched-precipitation ponds, being 215% larger than in the flow-through ponds (Table 3, Fig. 7). Most of the additional groundwater recharge occurs immediately following breakup. In the perched-precipitation ponds, stages are low when snow begins to fall, so there is a relatively large amount of accommodation space to trap aeolian-transported snow. This snow melts during breakup, and this surcharge of snow-melt water results in high stages immediately following breakup and enhanced groundwater recharge rates immediately thereafter (Table 3, Fig. 7). Conversely, in the flow-through ponds, stages are high when snow begins to fall, so there is a relatively small amount of accommodation space available to trap aeolian-transported snow. Lacking this surcharge of snow-melt water, high stages immediately following breakup and enhanced groundwater recharge immediately thereafter do not occur (Table 3, Fig. 7).

Both types of ponds differ from somewhat previously documented arctic ponds, most notably with respect to the roles that they play in groundwater recharge. In the early summer, inflows to arctic ponds are dominated by snowmelt, including overland flow from snowmelt that perches on still-frozen ground and flows overland toward topographic lows (Woo et al. 1981; Woo and Guan 2006). The trapping of aeolian-transported snow also appears to play an important role in arctic ponds, with snow accumulations being ~125% greater in arctic ponds than in the surrounding uplands (Woo et al. 1981). In the middle to late summer, inflows to arctic ponds are typically dominated by precipitation (Woo et al. 1981; Woo and Guan 2006), although the discharge of local, suprapermafrost ground water can occur depending upon local hydrogeologic and permafrost conditions (Kane and Slaughter 1973; Marsh and Woo 1977). Throughout the summer, outflows from arctic ponds are typically dominated by evapotranspiration (Marsh and Woo 1977; Woo and Guan 2006), although outburst flooding can play an important role during breakup if rapid inflows cause pond stages to abruptly rise and overtop and/or melt snow dams (Woo et al. 1981). Groundwater recharge does not appear to play an important role in arctic ponds, presumably due to the presence of permafrost aquitards (Marsh and Woo 1977; Woo et al. 1981; Woo and Guan 2006), although regional groundwater discharge and recharge can occur in deeper lakes with permafrost-free bottoms (Kane and Slaughter 1973).

Acknowledgments This project was funded by the Pebble Limited Partnership by way of a subcontract from Three Parameters Plus, Inc. Logistical and field support were provided by numerous people, most notably Cheryl Moody, Michael Exner-Kittridge, William Kleindl, Christopher Love, Karen Noyes, Christina Stringer, Brian Strong, and Rebecca Wachter, with Christopher Love playing a particularly important role in the earliest stages of project formulation and field data collection. Meteorological data were provided by Hoefler Consulting Group. Sarah Fratesi and Christina Stringer assisted in drafting Figs. 1 and 8. Kai Rains provided a critical review that greatly improved the manuscript.

References

Allen RG, Walter IA, Elliott RL, Howell TA, Itenfisu D, Jensen ME, Snyder RL (eds) (2005) The ASCE standardized reference evapotranspiration equation. American Society of Civil Engineers, Washington

Bauer HH, Mastin MC (1997) Recharge from precipitation in three small glacial-till-mantled catchments in the Puget Sound Lowland, Washington. US Geological Survey Water-Resources Investigations Report 96-4219. U.S. U.S. Government Printing Office, Washington

Born SM, Smith SA, Stephenson DA (1979) The hydrologic regime of glacial terrain lakes. Journal of Hydrology 43:7–44

Chamberlain EJ, Gow AJ (1979) Effect of freezing and thawing on the permeability and structure of soils. Engineering Geology 13:73–92

Clesceri LS, Greenberg AE, Eaton D (eds) (1998) Standard methods for the examination of water and wastewater, 20th edn. American Public Health Association, Washington

Corcoran RM, Lovvorn JR, Heglund PJ (2009) Long-term change in limnology and invertebrates in Alaskan boreal wetlands. Hydrobiologia 620:77–89

DeGraaf RM, Rappole JH (1995) Neotropical migratory birds: natural history, distribution, and population change. Cornell University Press, Ithaca

Dempster A, Ellis P, Wright B, Stone M, Price J (2006) Hydrogeological evaluation of a southern Ontario kettle-hole peatland and its linkage to a regional aquifer. Wetlands 26:49–56

Detterman RL, Reed BL (1973a) Surficial geology of the Iliamna Quadrangle, Alaska. U.S. Geological Survey Bulletin 1368-A. U. S. Government Printing Office, Washington

Detterman RL, Reed BL (1973b) Stratigraphy, structure, and economic geology of the Iliamna Quadrangle, Alaska. U.S. Geological Survey Bulletin 1368-B. U.S. U.S. Government Printing Office, Washington

Doorenbos J, Pruitt WO (eds.) (1977) Guidelines for prediction of crop water requirements. FAO Irrigation and Drainage Paper No. 24. Food and Agriculture Organization of the United Nations, Rome, Italy

Ferone JM, Devito KJ (2004) Shallow groundwater–surface water interactions in pond–peatland complexes along a Boreal Plains topographic gradient. Journal of Hydrology 292:75–95

Freeze RA, Cherry JA (1979) Groundwater. Prentice Hall, Englewood Cliffs

Gavilán P, Estévez J, Berengena J (2008) Comparison of standardized reference evapotranspiration equations in Southern Spain. Journal of Irrigation and Drainage Engineering 134:1–12

Hall JV, Frayer WE, Wilen BO (1994) The status of Alaska wetlands. U.S. Fish and Wildlife Service, Alaska Region, Anchorage, Alaska, USA

Hamilton TD, Klieforth RF (2010) Surficial geologic map of parts of the Iliamna D-6 and D-7 Quadrangles, Pebble project area, southwestern Alaska. Report of Investigations 2009-4. State of Alaska, Department of Natural Resources, Division of Geological and Geophysical Surveys, Fairbanks, Alaska, USA

Hanschke T, Baird AJ (2001) Time-lag errors associated with the use of simple standpipe piezometers in wetland soils. Wetlands 21:412–421

Johansson P-E (1987) Estimation of groundwater recharge in sandy till with two different methods using groundwater level fluctuations. Journal of Hydrology 90:183–198

Kane DL, Slaughter CW (1973) Recharge of a central Alaska lake by subpermafrost groundwater. In: Péwé TL, Mackay JR (eds) Permafrost, Second International Conference, North American Contribution, Yakutsk, USSR. National Academy of Sciences, Washington, pp 458–462

Karlstrom TNV (1964) Quaternary geology of the Kenai Lowlands and glacial history of the Cook Inlet Region, Alaska. US Geological Survey Professional Paper 443. U.S. Government Printing Office, Washington

Klein E, Berg EE, Dial R (2005) Wetland drying and succession across the Kenai Peninsula Lowlands, south-central Alaska. Canadian Journal of Forest Research 35:1931–1941

Labadia CF, Buttle JM (1996) Road salt accumulation in highway snow banks and transport through the unsaturated zone of the Oak Ridges Moraine, southern Ontario. Hydrological Processes 10:1575–1589

Mann DH, Peteet DM (1994) Extent and timing of the last glacial maximum in southwestern Alaska. Quaternary Research 42:136–148

Marsh P, Woo MK (1977) The water balance of a small pond in the High Arctic. Arctic 30:109–117

Meyboom P (1966) Unsteady groundwater flow near a willow ring in hummocky moraine. Journal of Hydrology 4:38–62

Parkhurst DL, Appelo CAJ (1999) User's guide to PHREEQC (Version 2)—a computer program for speciation, batch-reaction, one-dimensional transport, and inverse geochemical calculations. U.S. Geological Survey Water-Resources Investigations Report 99-4259. U.S. Government Printing Office, Washington, DC, USA

Péwé TL (1975) Quaternary geology of Alaska. U.S. Geological Survey Professional Paper 835. U.S. U.S. Government Printing Office, Washington

Prowse TD, Wrona FJ, Reist JD, Hobbie JE, Lévesque LMJ, Vincent WF (2006) General features of the arctic relevant to climate change in freshwater ecosystems. Ambio 35:330–338

Rains MC, Fogg GE, Harter T, Dahlgren RA, Williamson RJ (2006) The role of perched aquifers in hydrological connectivity and biogeochemical processes in vernal pool landscapes, Central Valley, California. Hydrological Processes 20:1157–1175

Richardson JL, Wilding LP, Daniels RB (1992) Recharge and discharge of groundwater in aquic conditions illustrated with flownet analysis. Geoderma 53:65–78

Saxena RK (1984) Seasonal variations of oxygen-18 in soil moisture and estimation of recharge in esker and moraine formations. Nordic Hydrology 15:235–242

Sloan CE (1972) Ground-water hydrology of prairie potholes in North Dakota. U.S. Geological Survey Professional Paper 585-C. U.S. Government Printing Office, Washington

Smith R (2009a) Water Resources Consultants. E-mail to MC Rains with appended data analysis. June 9

Smith R (2009b) Water Resources Consultants. E-mail to MC Rains with appended data analysis. May 21

State of Alaska (2004) Alaska's outdoor legacy: statewide comprehensive outdoor recreation plan (SCORP) 2004–2009. Department of Natural Resources and Division of Parks and Outdoor Recreation, Juneau, Alaska, USA

Stilwell KB, Kaufman DS (1996) Late-Wisconsin glacial history of the northern Alaska Peninsula, southwestern Alaska, U.S.A. Arctic and Alpine Research 28:475–487

Sumner DM (2007) Effects of capillarity and microtopography on wetland specific yield. Wetlands 27:693–701

Todd AK, Buttle JM, Taylor CH (2006) Hydrologic dynamics and linkages in a wetland-dominated basin. Journal of Hydrology 319:15–35

van der Kamp G, Hayashi M (1998) The groundwater recharge function of small wetlands in the semi-arid northern prairies. Great Plains Research 8:39–56

Ventura F, Spano D, Duce P, Snyder RL (1999) An evaluation of common evapotranspiration equations. Irrigation Science 18:163–170

Viereck LA, Dyrness CT, Batten AR, Wenzlick KJ (1992) The Alaska vegetation classification. General Technical Report PNW-GTR-286. U.S. Department of Agriculture, Forest Service, Pacific Northwest Research Station, Portland, Oregon, USA

Wahrhaftig C (1965) Physiographic divisions of Alaska. U.S. Geological Survey Professional Paper 482. U.S. Government Printing Office, Washington, DC, USA

Woo M-K, Guan XJ (2006) Hydrological connectivity and seasonal storage change of tundra ponds in a polar oasis environment, Canadian High Arctic. Permafrost and Periglacial Processes 17:309–323

Woo M-K, Heron R, Steet P (1981) Catchment hydrology of a High Arctic lake. Cold Regions Science and Technology 5:29–41